

Kosuke Ito,<sup>a\*</sup> Hao Qi,<sup>b</sup> Yoshihiro Shimizu,<sup>b</sup> Ryo Murakami,<sup>a</sup> Kin-ichiro Miura,<sup>b</sup> Takuya Ueda<sup>b</sup> and Toshio Uchiumi<sup>a</sup>

<sup>a</sup>Department of Biology, Faculty of Science, Niigata University, 8050 Ikarashi 2-no-cho, Nishi-ku, Niigata 950-2181, Japan, and <sup>b</sup>Department of Medical Genome Sciences, Graduate School of Frontier Sciences, University of Tokyo, 5-1-5 Kashiwanoha, Kashiwa, Chiba 277-8562, Japan

Correspondence e-mail:  
k-ito@bio.sc.niigata-u.ac.jp

Received 12 May 2011  
Accepted 19 September 2011

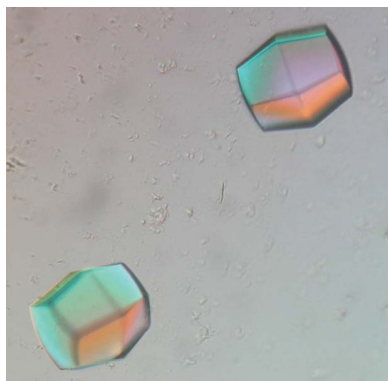
## Crystallization and preliminary X-ray analysis of peptidyl-tRNA hydrolase from *Escherichia coli* in complex with the acceptor-TΨC domain of tRNA

Peptidyl-tRNA hydrolase (Pth) cleaves the ester bond between the peptide and the tRNA of peptidyl-tRNA molecules, which are the product of aborted translation. In the present work, Pth from *Escherichia coli* was crystallized with the acceptor-TΨC domain of tRNA using 1,4-butanediol as a precipitant. The crystals belonged to the hexagonal space group  $P6_1$ , with unit-cell parameters  $a = b = 55.1$ ,  $c = 413.1$  Å, and diffracted X-rays beyond 2.4 Å resolution. The asymmetric unit is expected to contain two complexes of Pth and the acceptor-TΨC domain of tRNA ( $V_M = 2.8$  Å<sup>3</sup> Da<sup>-1</sup>), with a solvent content of 60.8%. The structure is being solved by molecular replacement.

### 1. Introduction

During the course of protein synthesis, peptidyl-tRNA is prematurely produced from the ribosome as a result of aborted translation (Menninger, 1976). The accumulation of peptidyl-tRNA limits the amount of free tRNA for protein synthesis; therefore, such an accumulation is toxic to cells (Atherly, 1978; Menninger, 1979). This situation is prevented by the activity of peptidyl-tRNA hydrolase (Pth), which releases tRNA from peptidyl-tRNA by cleaving the ester bond between the C-terminal end of the peptide and the 2'- or 3'-hydroxyl of the ribose at the 3' end of the tRNA (Cuzin *et al.*, 1967; Kössel & RajBhandary, 1968; Das & Varshney, 2006). Pth is ubiquitous in nature and can be classified into two types: Pth, which is sometimes referred to as Pth1, and Pth2. Pth exists in bacteria and eukaryotes (Kössel, 1970; Brun *et al.*, 1971; Menez *et al.*, 2002), whereas Pth2 is present in eukaryotes and archaea (Rosas-Sandoval *et al.*, 2002; Fromant *et al.*, 2003). Despite a lack of sequence similarity, the two enzyme classes have similar biological activities. Indeed, *Escherichia coli* strains lacking endogenous Pth are rescued by the expression of Pth2 (Rosas-Sandoval *et al.*, 2002; Fromant *et al.*, 2003). The activity of Pth is known to be essential for the viability of bacteria (Atherly & Menninger, 1972; Menez *et al.*, 2002).

The biochemical features of *E. coli* Pth have been well studied. N-blocked aminoacyl-tRNAs are the shortest substrates of the enzyme (Cuzin *et al.*, 1967; Kössel & RajBhandary, 1968); however, N-formylmethionyl-tRNA<sup>Met</sup> is resistant to attack by Pth (Kössel & RajBhandary, 1968; Kössel, 1970). Indeed, formylated initiator tRNA must be kept intact in order to participate in the formation of the ribosomal initiator complex. This resistance is thought to be a consequence of the lack of base pairing at position 1–72 in tRNA<sup>Met</sup>, which may cause incorrect positioning of the 5'-phosphate that is necessary for Pth activity (Schulman & Pelka, 1975; Dutka *et al.*, 1993). However, the molecular mechanism of this substrate discrimination remains unknown. In contrast, Pth can accept many kinds of peptidyl or N-blocked aminoacyl-elongator tRNAs (Kössel & RajBhandary, 1968; de Groot *et al.*, 1969). The enzyme recognizes both the peptidic and the nucleotidic moieties of the substrate



(Shiloach *et al.*, 1975), both of which consist of various sequences depending on the substrate. The mechanism for this broad substrate specificity also remains unknown.

The structures of Pth from *E. coli* (Schmitt, Mechulam *et al.*, 1997), *Mycobacterium tuberculosis* (Selvaraj *et al.*, 2007; Pulavarti *et al.*, 2008) and *Francisella tularensis* (Clarke *et al.*, 2011) have been determined. Structures of Pth2 from *Homo sapiens* (de Pereda *et al.*, 2004), *Sulfolobus solfataricus* (Fromant *et al.*, 2005), *Archaeoglobus fulgidis* (Powers *et al.*, 2005) and *Pyrococcus horikoshii* (Shimizu *et al.*, 2008) have also been reported. In combination with biochemical experiments, these structural studies have enabled us to predict the catalytic residues and substrate-recognition regions of the enzymes. Because all of these structures have been determined in the apo form, however, the molecular mechanism of the reaction remains unclear. Thus, as a first step towards elucidating this mechanism, we attempted to crystallize *E. coli* Pth with full-length tRNA, a competitive inhibitor of Pth (Shiloach *et al.*, 1975). In addition, we attempted to crystallize *E. coli* Pth with the acceptor-T $\Psi$ C domain of tRNA, because the enzyme has been predicted to bind to the tRNA moiety of the substrate through this region (Fromant *et al.*, 1999) and this region is thought to be structurally stable. Here, we report sample preparation, crystallization and preliminary X-ray crystallographic analysis. This is the first report of the crystallization of Pth in complex with its ligand.

## 2. Materials and methods

### 2.1. Preparation of full-length tRNA

The pET vector containing the full-length mature *E. coli* tRNA<sup>Ala</sup><sub>GGC</sub> sequence was a gift from Dr Takashi Yokogawa (Gifu University, Japan). A template for *in vitro* transcription was obtained by PCR with the above vector and the following pair of oligo DNAs: 5'-GAAATTAATACGACTCACTATAGGGGCTATAGCTCAGCTGGGA-3' and 5'-TmGGTGGAGCTAAGCGGGATCG-3'. The T7 RNA polymerase promoter sequence is represented in bold. mG represents the 2'-*O*-methyl nucleotide, which is used to manipulate the uniform 3' ends of transcribed products (Sherlin *et al.*, 2001). To obtain tRNA bearing a monophosphorylated guanosine at the 5' terminus, the RNA was synthesized by *in vitro* transcription using T7 RNA polymerase in the presence of a tenfold molar excess of GMP over GTP. The transcribed product was purified by phenol/chloroform treatment. The product was dialyzed against buffer consisting of 20 mM HEPES-KOH pH 7.6, 200 mM KCl. For renaturation, the solution was heated at 343 K for 5 min, followed by the addition of MgCl<sub>2</sub> to 10 mM and gradual cooling to 298 K. The sample was further purified on a HiTrap Q HP column (GE Healthcare), using 20 mM HEPES-KOH pH 7.6 containing 150 mM KCl as a starting buffer, with a linear gradient of 150–1000 mM KCl. Finally, the RNA was exchanged to buffer A (10 mM HEPES-KOH pH 7.6 containing 10 mM MgCl<sub>2</sub> and 7 mM  $\beta$ -mercaptoethanol) and concentrated using a Vivaspin centrifugal concentrator (3 kDa cutoff; Sartorius). The sample was stored at 193 K prior to use.

### 2.2. Preparation of the acceptor-T $\Psi$ C domain of tRNA

The DNA fragment encoding the acceptor-T $\Psi$ C domain of the *E. coli* tRNA<sup>Ala</sup><sub>GGC</sub> gene, with the preceding sequence of the T7 RNA polymerase promoter (GAAATTAATACGACTCACTATAGGGGCTAAGCGGTTTCGATCCCGCTTAGCTCCACCA, in which the T7 RNA polymerase promoter sequence is represented in bold), was PCR-amplified and cloned into the pUC18 vector. A template for *in vitro* transcription was obtained by PCR with the above vector and

the following pairs of oligo DNAs: 5'-GAAATTAATACGACTCACTATAG-3' and 5'-TmGGTGGAGCTAAGCGGGATCG-3'. mG represents the 2'-*O*-methyl nucleotide, which is used for manipulating the uniform 3' end of transcribed products (Sherlin *et al.*, 2001). *In vitro* transcription and purification were performed in a manner similar to that for full-length tRNA.

### 2.3. Overexpression and purification of *E. coli* Pth

A method for the purification of *E. coli* Pth has been reported previously (Dutka *et al.*, 1993; Schmitt, Fromant *et al.*, 1997); however, we purified this enzyme more easily and effectively with a His tag as follows. The gene encoding *E. coli* Pth was PCR-amplified and cloned into the pET-15b vector (Novagen). The recombinant protein was overexpressed in *E. coli* strain BL21 (DE3) (Novagen) with an N-terminal His tag and a thrombin cleavage site (MGSSHHHHH-HSSGLVPR/GSH, where / represents the thrombin cleavage site). After sonication of *E. coli* cells in buffer B (50 mM HEPES-KOH pH 7.6 containing 1 M ammonium chloride and 7 mM  $\beta$ -mercaptoethanol), the clarified lysate was loaded onto a HisTrap HP column (GE Healthcare) equilibrated with buffer B. His-tagged Pth was eluted with a linear gradient to 50 mM HEPES-KOH buffer pH 7.6 containing 100 mM KCl, 7 mM  $\beta$ -mercaptoethanol and 200 mM imidazole. The His-tagged Pth was then cleaved by the addition of thrombin. The protease was inactivated and removed by adding Benzamidine Sepharose 4 Fast Flow (high sub; GE Healthcare), followed by filtration. To remove isolated His tag and undigested His-tagged Pth from untagged Pth, the protein solution was diluted four times with buffer B and loaded onto an Ni-NTA agarose (Qiagen) column equilibrated with buffer B. The flowthrough fraction was then collected and dialyzed against buffer C (10 mM HEPES-KOH pH 7.6 containing 7 mM  $\beta$ -mercaptoethanol). Subsequently, to absorb residual contaminant proteins, the flowthrough fraction of the Ni-NTA agarose column was loaded onto a Q Sepharose Fast Flow (GE Healthcare) column equilibrated with buffer C. The flowthrough fraction was collected and concentrated using an Amicon Ultra centrifugal concentrator (10 kDa cutoff, Millipore). The sample was stored at 193 K prior to use.

### 2.4. Crystallization and X-ray data collection

Initial crystallization trials were performed by the sitting-drop vapour-diffusion method using Crystal Screen, Crystal Screen 2, Crystal Screen Lite, Natrix (Hampton Research) and Wizard I and II (Emerald BioSystems). Pth and full-length tRNA or the acceptor-T $\Psi$ C domain of tRNA were mixed in buffer A in a 1:2 molar ratio with a final Pth concentration of 7 mg ml<sup>-1</sup>. The mixture was heated at 310 K for 10 min and gradually cooled to 298 K. Sitting drops were prepared by mixing 1  $\mu$ l sample solution with an equal volume of reservoir solution and were equilibrated against 50  $\mu$ l reservoir solution in a 96-well plate at 293 K. Trials to improve the crystallization conditions were performed by varying the pH, temperature, precipitant concentration, protein concentration, molar ratio of protein to RNA and sample and reservoir solution volumes, as well as by the use of Additive Screen (Hampton Research). All of these trials were performed by the sitting-drop vapour-diffusion method using 24-well plates and the drops were equilibrated against 450  $\mu$ l reservoir solution.

For data collection under cryogenic conditions, crystals were mounted in nylon loops (Hampton Research), transferred into a reservoir solution containing ethylene glycol and flash-cooled in a stream of nitrogen. X-ray diffraction data were collected at 100 K on the BL41XU beamline at SPring-8 (Harima, Japan) using a MAR 225

CCD detector. Diffraction data were processed and scaled using *XDS* (Kabsch, 2010); other crystallographic calculations were carried out with the *CCP4* package (Winn *et al.*, 2011).

### 3. Results and discussion

Pth was overexpressed and purified with a yield of 110 mg protein from 1 l culture. The purity of the protein was estimated to be greater than 95% by SDS-PAGE. Full-length tRNA and the acceptor-T $\Psi$ C domain of tRNA were synthesized by *in vitro* transcription with T7 RNA polymerase. The purity of the RNA was estimated to be greater than 90% by urea PAGE.

We could not obtain crystals of Pth in complex with full-length tRNA from the initial crystallization trials. We think that flexible structural features of the tRNA might cause problems in crystallization. In contrast, microcrystals of less than 10  $\mu$ m were obtained

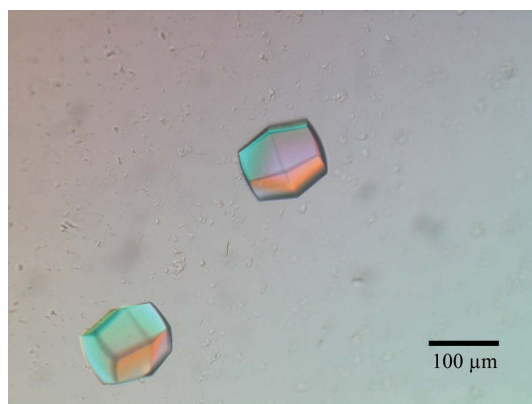


**Figure 1**  
Crystals of *E. coli* Pth in complex with the acceptor-T $\Psi$ C domain of tRNA. The average dimensions of these crystals were 100  $\times$  100  $\times$  30  $\mu$ m.

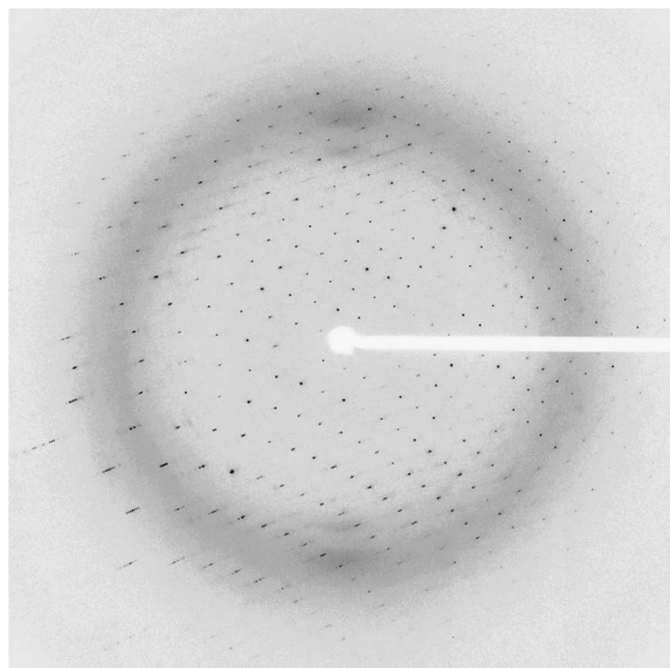


**Figure 2**  
X-ray diffraction image of a crystal of *E. coli* Pth in complex with the acceptor-T $\Psi$ C domain of tRNA. The edge of the detector corresponds to a resolution of 2.4  $\text{\AA}$ .

**Table 1**  
Crystal data, data-collection and processing statistics.

Values in parentheses are for the highest resolution shell.

Crystal data	
Crystal dimensions ( $\mu$ m)	100 $\times$ 100 $\times$ 30
Space group	$P6_1$
Unit-cell parameters ( $\text{\AA}$ )	$a = b = 55.1$ , $c = 413.1$
No. of complexes per asymmetric unit	2
$V_M$ ( $\text{\AA}^3 \text{Da}^{-1}$ )	2.8
Solvent content (%)	60.8
Data collection and processing	
Beamline	BL41XU, SPring-8
Detector	MAR 225 CCD
Wavelength ( $\text{\AA}$ )	1.000
X-ray beam size (mm)	0.05 $\times$ 0.05
Crystal-to-detector distance (mm)	270
Oscillation angle ( $^\circ$ )	0.4
Total oscillation range ( $^\circ$ )	180
Temperature (K)	100
Resolution range ( $\text{\AA}$ )	50.0–2.40 (2.54–2.40)
No. of measured reflections	296148 (33377)
No. of unique reflections	27129 (4136)
Completeness (%)	98.1 (93.7)
Multiplicity	10.9 (8.1)
Average $I/\sigma(I)$	24.9 (8.2)
$R_{\text{merge}}^\dagger$	0.056 (0.187)
Data-processing software	<i>XDS</i>

$^\dagger R_{\text{merge}} = \frac{\sum_{hkl} \sum_i |I_i(hkl) - \langle I(hkl) \rangle|}{\sum_{hkl} \sum_i I_i(hkl)}$ , where  $I_i(hkl)$  is the  $i$ th intensity measurement of reflection  $hkl$ , including symmetry-related reflections, and  $\langle I(hkl) \rangle$  is its average.

with Wizard I condition No. 35 [100 mM acetate buffer pH 4.5, 20% (w/v) 1,4-butanediol] in the case of initial crystallization trials with the acceptor-T $\Psi$ C domain of tRNA, which is thought to be structurally more stable than full-length tRNA. No other crystallization conditions were found in the initial trials. As a result of refining these crystallization conditions, crystals suitable for X-ray analysis were obtained by the sitting-drop vapour-diffusion method by mixing 1  $\mu$ l sample solution (with a 1:2.5 molar ratio of Pth to the acceptor-T $\Psi$ C domain of tRNA and a final Pth concentration of 14 mg ml $^{-1}$ ) and 1  $\mu$ l reservoir solution consisting of 100 mM acetate buffer pH 5.2, 20% (w/v) 1,4-butanediol and 30 mM glycyl-glycyl-glycine. The crystals grew within two weeks to maximum dimensions of 100  $\times$  100  $\times$  30  $\mu$ m at 293 K (Fig. 1). No crystals were obtained when a sample solution containing only protein or RNA was used, suggesting that the crystals contained both Pth and the acceptor-T $\Psi$ C domain of tRNA. We will provide further evidence that the crystals contain both Pth and the acceptor-T $\Psi$ C domain of tRNA. It is interesting that glycyl-glycyl-glycine significantly improved the size of the crystals, as a peptide is a product of the Pth reaction. Binding of glycyl-glycyl-glycine to the active site may influence the conformation of the enzyme and the crystal packing.

Diffraction data were collected from a cryocooled crystal using a MAR 225 CCD detector on BL41XU at SPring-8. Ice-ring formation was prevented by using reservoir solution containing 10% (v/v) ethylene glycol. The wavelength was set to 1.000  $\text{\AA}$ , the oscillation angle was set to 0.4 $^\circ$  and the crystal-to-detector distance was set to 270 mm. The crystals diffracted X-rays to beyond 2.4  $\text{\AA}$  resolution (Fig. 2). Analysis of merging statistics and systematic absences indicated that the crystals belonged to the hexagonal space group  $P6_1$  or  $P6_5$ , with unit-cell parameters  $a = b = 55.1$ ,  $c = 413.1$   $\text{\AA}$ . Under the assumption that the crystals were a complex of Pth and the acceptor-T $\Psi$ C domain of tRNA, the crystals were expected to contain two complexes per asymmetric unit, corresponding to a solvent content of 60.8% and a Matthews coefficient  $V_M$  (Matthews, 1968) of 2.8  $\text{\AA}^3 \text{Da}^{-1}$  (the molecular weight of Pth is 21.1 kDa and that of the acceptor-T $\Psi$ C domain of tRNA is 11.2 kDa). Indeed, these crystals

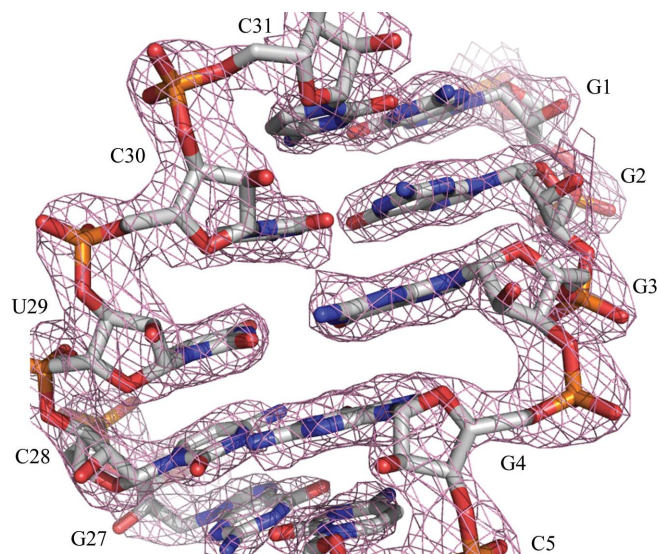


**Figure 3**

$\sigma_A$ -weighted  $2F_o - F_c$  electron-density map surrounding part of the acceptor-TΨC domain of tRNA. The map is contoured at  $1.5\sigma$ . The molecule is shown as a stick model, with C atoms in grey, O atoms in red, N atoms in blue and P atoms in orange. The figure was prepared with *PyMOL* (DeLano, 2002).

included both components (see below). The data-collection statistics are summarized in Table 1.

In order to solve the structure, molecular replacement with *MOLREP* (Vagin & Teplyakov, 2010) was attempted using the structure of *E. coli* Pth (PDB code 2pth; Schmitt, Mechulam *et al.*, 1997) as a search model, which produced a clear solution. The space group was determined to be  $P6_1$ . The electron density of the acceptor-TΨC domain of tRNA was then obtained by phase improvement with *ARP/wARP* (Perrakis *et al.*, 1999) and initial model building of the acceptor-TΨC domain of tRNA was able to proceed automatically with *PHENIX* (Adams *et al.*, 2002; Fig. 3). These results showed that the crystals obtained were a complex of Pth and the acceptor-TΨC domain of tRNA. Structure refinement is now in progress.

We would like to thank Dr Min Yao, Hokkaido University for helpful advice during data collection. The synchrotron-radiation experiments were performed on BL41XU at SPring-8 (Harima, Japan) with the approval of the Japan Synchrotron Radiation Research Institute (Proposal No. 2008B2182). This work was supported in part by Grants-in-Aid for Young Scientists (Start-up) 20870018 and (B) 21770108 from the Japan Society for the Promotion of Science (JSPS; to KI) and by grant 22-1-10 from the Uchida Energy Science Promotion Foundation (to KI).

## References

- Adams, P. D., Grosse-Kunstleve, R. W., Hung, L.-W., Ioerger, T. R., McCoy, A. J., Moriarty, N. W., Read, R. J., Sacchettini, J. C., Sauter, N. K. & Terwilliger, T. C. (2002). *Acta Cryst.* **D58**, 1948–1954.
- Atherly, A. G. (1978). *Nature (London)*, **275**, 769.
- Atherly, A. G. & Menninger, J. R. (1972). *Nature New Biol.* **240**, 245–246.
- Brun, G., Paulin, D., Yot, P. & Chapeville, F. (1971). *Biochimie*, **53**, 225–231.
- Clarke, T. E., Romanov, V., Lam, R., Gothe, S. A., Peddi, S. R., Razumova, E. B., Lipman, R. S. A., Branstrom, A. A. & Chirgadze, N. Y. (2011). *Acta Cryst.* **F67**, 446–449.
- Cuzin, F., Kretschmer, N., Greenberg, R. E., Hurwitz, R. & Chapeville, F. (1967). *Proc. Natl Acad. Sci. USA*, **58**, 2079–2086.
- Das, G. & Varshney, U. (2006). *Microbiology*, **152**, 2191–2195.
- De Groot, N., Groner, Y. & Lapidot, Y. (1969). *Biochim. Biophys. Acta*, **186**, 286–296.
- DeLano, W. L. (2002). *PyMOL*. <http://www.pymol.org>.
- De Pereda, J. M., Waas, W. F., Jan, Y., Ruoslahti, E., Schimmel, P. & Pascual, J. (2004). *J. Biol. Chem.* **279**, 8111–8115.
- Dutka, S., Meinel, T., Lazennec, C., Mechulam, Y. & Blanquet, S. (1993). *Nucleic Acids Res.* **21**, 4025–4030.
- Fromant, M., Ferri-Fioni, M. L., Plateau, P. & Blanquet, S. (2003). *Nucleic Acids Res.* **31**, 3227–3235.
- Fromant, M., Plateau, P., Schmitt, E., Mechulam, Y. & Blanquet, S. (1999). *Biochemistry*, **38**, 4982–4987.
- Fromant, M., Schmitt, E., Mechulam, Y., Lazennec, C., Plateau, P. & Blanquet, S. (2005). *Biochemistry*, **44**, 4294–4301.
- Kabsch, W. (2010). *Acta Cryst.* **D66**, 125–132.
- Kössel, H. (1970). *Biochim. Biophys. Acta*, **204**, 191–202.
- Kössel, H. & RajBhandary, U. L. (1968). *J. Mol. Biol.* **35**, 539–560.
- Matthews, B. W. (1968). *J. Mol. Biol.* **33**, 491–497.
- Menez, J., Buckingham, R. H., de Zamaroczy, M. & Campelli, C. K. (2002). *Mol. Microbiol.* **45**, 123–129.
- Menninger, J. R. (1976). *J. Biol. Chem.* **251**, 3392–3398.
- Menninger, J. R. (1979). *J. Bacteriol.* **137**, 694–696.
- Perrakis, A., Morris, R. & Lamzin, V. S. (1999). *Nature Struct. Biol.* **6**, 458–463.
- Powers, R., Mirkovic, N., Goldsmith-Fischman, S., Acton, T. B., Chiang, Y., Huang, Y. J., Ma, L., Rajan, P. K., Cort, J. R., Kennedy, M. A., Liu, J., Rost, B., Honig, B., Murray, D. & Montelione, G. T. (2005). *Protein Sci.* **14**, 2849–2861.
- Pulavarti, S. V., Jain, A., Pathak, P. P., Mahmood, A. & Arora, A. (2008). *J. Mol. Biol.* **378**, 165–177.
- Rosas-Sandoval, G., Ambrogelly, A., Rinehart, J., Wei, D., Cruz-Vera, L. R., Graham, D. E., Stetter, K. O., Guarneros, G. & Söll, D. (2002). *Proc. Natl Acad. Sci. USA*, **99**, 16707–16712.
- Schmitt, E., Fromant, M., Plateau, P., Mechulam, Y. & Blanquet, S. (1997). *Proteins*, **28**, 135–136.
- Schmitt, E., Mechulam, Y., Fromant, M., Plateau, P. & Blanquet, S. (1997). *EMBO J.* **16**, 4760–4769.
- Schulman, L. H. & Pelka, H. (1975). *J. Biol. Chem.* **250**, 542–547.
- Selvaraj, M., Roy, S., Singh, N. S., Sangeetha, R., Varshney, U. & Vijayan, M. (2007). *J. Mol. Biol.* **372**, 186–193.
- Sherlin, L. D., Bullock, T. L., Nissan, T. A., Perona, J. J., Lariviere, F. J., Uhlenbeck, O. C. & Scaringe, S. A. (2001). *RNA*, **7**, 1671–1678.
- Shiloach, J., Bauer, S., de Groot, N. & Lapidot, Y. (1975). *Nucleic Acids Res.* **2**, 1941–1950.
- Shimizu, K., Kuroishi, C., Sugahara, M. & Kunishima, N. (2008). *Acta Cryst.* **D64**, 444–453.
- Vagin, A. & Teplyakov, A. (2010). *Acta Cryst.* **D66**, 22–25.
- Winn, M. D. *et al.* (2011). *Acta Cryst.* **D67**, 235–242.